

Mean-field coupling of calcium oscillations in a multicellular system of rat hepatocytes

Dan Wu, Ya Jia *

Department of Physics and Institute of Biophysics, Central China Normal University, Wuhan 430079, China

Received 27 April 2006; received in revised form 15 August 2006; accepted 16 August 2006

Available online 22 August 2006

Abstract

In a multicellular system of rat hepatocytes and even in an intact liver, cytoplasmic calcium oscillations are synchronized and highly coordinated. In this paper, the mean-field coupling term has been introduced to describe the coupling flux, which is more efficient than gap junctional coupling terms. An optimal coupling strength and an optimal stimulation level for the synchronization of the coupled system have been observed in this paper. Moreover, it has been proved that these results are independent of the cells number. Interestingly, it has been observed that the intracellular noise and the extracellular noise have different effects on the synchronization of the coupled system.
© 2006 Elsevier B.V. All rights reserved.

Keywords: Mean-field coupling; Synchronization; Coupling strength; Stimulation level; Ca^{2+} channel number; Cells number

1. Introduction

It is well known that biochemical oscillations are encountered at all levels of biological organization [1]. Isolated hepatocytes as well as many other cells, exhibit cytoplasmic Ca^{2+} oscillations upon the stimulation with low concentrations of IP_3 (inositol 1,4,5-triphosphate)-dependent agonists [2,3]. Cytoplasmic Ca^{2+} oscillations in hepatocytes play important roles in regulation of many intracellular physiological processes [4–8]. For example, Ca^{2+} regulates phosphorylation–dephosphorylation cycle process involved in glycogen degradation, which had been investigated theoretically [9–11].

On the smaller scale of isolated hepatocyte couplets, cytoplasmic Ca^{2+} oscillations in adjacent cells demonstrate near-synchrony coordination [12]. This coordination has been extensively investigated from both experimental [12–14] and theoretical [15–19] points. Considering that many theoretical studies have ignored effects of IP_3 level (an important second messenger, can combine and activate Ca^{2+} channels on endoplasmic reticulum, ER), we have investigated effects of the IP_3 level and the coupling strength on synchrony of Ca^{2+} oscillations in two coupled cells [18]. It has been found that: gap

junctions permeable to calcium and to IP_3 both are effective on synchronizing Ca^{2+} oscillations in coupled hepatocytes; the relationship between locking rates of Ca^{2+} oscillations and coupling strength reveals a devils staircase-like structure, which demonstrates that there exist both 1:1 phase locking and various harmonic-locking of intercellular Ca^{2+} oscillations; cross-correlation analysis suggests that there exist optimal coupling strength and IP_3 level to obtain the most orderly coupled system. Because there are few investigations about stochastic effects and noise strength in coupled hepatocytes, we have explored effects of noise on synchrony of stochastic Ca^{2+} oscillations in two and three coupled cells [19]. It has been found that: with the increasing of coupling strength, the interspike interval (ISI), phase difference ($\Delta\phi$), cyclic relative phase (Φ) and its distribution all transform from unsynchronized state to synchronized one; signal-to-noise ratio in two parameters space (coupling strength–total Ca^{2+} channel number) suggests that there exists coherence resonance for two and three coupled hepatocytes.

Previous studies focus on coupled hepatocytes with small cells number [15–19], however, in an intact liver, Robbgaspers and Thomas [20] and Nathanson et al. [21] found that cytoplasmic Ca^{2+} oscillations evoked by IP_3 linked agonists were organized as coordinated periodic waves across whole liver lobules (about 500 cells). For a biological system that coupled by many elements,

* Corresponding author.

E-mail address: wud@phy.ccnu.edu.cn (D. Wu).

coupling terms denoted by gap junctional fluxes are complex and low efficient. Now a question to be raised is that if there exist another efficient and correct description to deal with a coupled multicellular system? In this paper, a global coupling flux described by a mean-field term has been introduced, which had been used in coupled circadian oscillators [22], to our knowledge, has never been used in calcium dynamics. Considering that a liver lobule always present sixangles prism with 2 mm length and 0.1 mm width, calcium wave propagates at a velocity of $50\text{--}150\text{ }\mu\text{m s}^{-1}$ [20,21] through the whole liver lobule (about 500 cells) in 1–20 s. Moreover, in this paper, calcium oscillates in individual cell at a period of 13–25 s. Based on the above-mentioned reasons, we assumed that the release of cytoplasmic calcium is supposed to become homogenous to establish an average calcium level. It is a reasonable theoretical hypothesis to consider global coupling, achieved through a mean field, defined as the average concentration of cytoplasmic calcium. Our findings in the article proved that a mean field approach can be an effective way to couple a population of hepatocyte's calcium oscillators.

In this paper, effects of the coupling strength and the stimulation level on the synchronization of the coupled system have been theoretically explored. The system studied here is composed of 500 hepatocytes: a typical cells number of whole liver lobules [21]. The order parameter O , the degree of the phase synchronization S and the coherence of oscillations R have been applied to measure the synchronization of the coupled system. The results obtained by this different definition are consistent. There exist optimal coupling strength and stimulation level for the synchronization of this system. Moreover, these results are proved to be independent of the cells number. Interestingly, it has been found that the intracellular noise and the extracellular noise have different effects on the synchronization of the system. The former tends to make the system disorder, and the latter exerts more complex influence on the system.

2. Model

Our simulation is based on Höfer's model [16] and employs stochastic Li–Rinzel model [23] to describe the channel flux. The stochastic opening and closing of calcium channels are described by Langevin method [24]. To consider the stochastic Ca^{2+} oscillations in coupled hepatocytes and effects of the IP_3 level, the model has been made some changes (see Refs. [18,19] for details).

The balance equations for the concentration of cytoplasmic-free calcium and the free calcium content of the whole cell in the i th cell (x_i and z_i , respectively) are given by:

$$\frac{dx_i}{dt} = \rho(J_{\text{in}} - J_{\text{out}} + \alpha(J_{\text{rel}} - J_{\text{SERCA}}) + J_{\text{coupling}}), \quad (1)$$

$$\frac{dz_i}{dt} = \rho(J_{\text{in}} - J_{\text{out}} + J_{\text{coupling}}). \quad (2)$$

The index i denotes the i th cell, $i = 1, 2, \dots, N$. A conservation of the total cellular Ca^{2+} implies the constraint: $z_i = x_i + \beta y_i$. y_i

denotes the free calcium concentration in the ER (endoplasmic reticulum) of the i th cell. ρ , α and β are structural characteristics of the cell. Expressions for these fluxes are:

$$J_{\text{in}} = v_0 + v_c \frac{P_i}{K_0 + P_i},$$

$$J_{\text{out}} = v_4 \frac{x_i^2}{K_4^2 + x_i^2},$$

$$J_{\text{SERCA}} = v_3 \frac{x_i^2}{K_3^2 + x_i^2},$$

$$J_{\text{rel}} = (k_1 m_\infty^3 n_\infty^3 h^3 + k_2)(y_i - x_i).$$

The expression of the coupling term is based on the definition of the global coupling term in Ref. [22]. Moreover, $v_c \frac{P_i}{K_0 + P_i}$ in the expression of the flux J_{in} (through the plasm membrane from extracellular space into cytoplasm) has a similar structure. The evolutions of x_i and P_i is almost in phase [18]. Therefore, the coupling term J_{coupling} is described by:

$$J_{\text{coupling}} = c \frac{\gamma F}{A + \gamma F}$$

The parameter γ describes the sensitivity of the individual cell to environment and is referred below as the coupling strength. If taking $\gamma = 0$, Eqs. (1) and (2) describe the dynamical behavior of isolated cells. In this paper, an average cytoplasmic calcium level, or a mean-field F is established as:

$$F(t) = \frac{1}{N} \sum_{i=1}^N x_i(t)$$

P_i denotes the intracellular IP_3 concentration in the i th cell. We have incorporated a general equation in this model to describe the synthesis of IP_3 by phospholipase C (PLC) and the IP_3 metabolism by IP_3 3-kinase and 5-phosphatase [25]:

$$\frac{dP_i}{dt} = V_{\text{PLC}} - V_K \frac{P_i}{K_K + P_i} \frac{x_i^2}{K_d + x_i^2} - V_{\text{PH}} \frac{P_i}{K_{\text{PH}} + P_i} \quad (3)$$

where V_{PLC} is the velocity of IP_3 synthesized by PLC. Because that parameter V_{PLC} depends on the stimulation level, V_{PLC} is referred below as a measurement of the stimulation level.

This model assumes that three equivalent and independent subunits are involved in conduction in an IP_3 receptor. Each subunit has one IP_3 binding site (m gates), and two Ca^{2+} binding sites (one for activation (n gates), the other for inhibition (h gates)). The fast variables m , n can be replaced by their quasi-equilibrium values m_∞ ($m_\infty = \frac{P}{d_P + P}$) and n_∞ ($n_\infty = \frac{x}{d_a + x}$) [23]. The opening and closing of h gates in each

IP₃ receptor are much slower than those of the other two gates. The random opening and closing of these channels introduce stochasticity into the calcium release mechanism. The Langevin equation for the fraction of h-open gates is then expressed as [24]:

$$\frac{dh}{dt} = \alpha_h(1-h) - \beta_h h + G_h(t) \quad (4)$$

where $G_h(t)$ is zero mean, uncorrelated, Gaussian white noise terms with

$$\langle G_h(t)G_h(t') \rangle = \frac{\alpha_h(1-h) + \beta_h h}{M} \delta(t-t')$$

α_h ($\alpha_h = d_2 \frac{P+d_1}{P+d_3}$) and β_h ($\beta_h = x$) are opening rate and closing rate for h gates respectively. M indicates the total number of IP₃R channels those locate on ER in one cell. For a multicellular system, the structure of each cell is not identical. Höfer [16] had investigated the synchronization of two coupled heterogeneous hepatocytes and 3 had studied the effects of the degree of heterogeneity. Therefore a small noise is introduced into the structure parameter β to consider the heterogeneity of cells:

$$\beta = \beta_0(1 + \xi(i))$$

$\xi(i)$ is the Gaussian noise with zero mean value and its correlation function is: $\langle \xi(i)\xi(j) \rangle = \sigma^2 \delta_{ij}$, where σ denotes the noise intensity (here σ is set as 2.0). The values of these parameters [15,18] are: $\rho=0.02$, $\alpha=2.0$, $\beta_0=0.1$, $v_0=0.2 \mu\text{M s}^{-1}$, $v_c=4.0 \mu\text{M s}^{-1}$, $v_3=9.0 \mu\text{M s}^{-1}$, $v_4=3.6 \mu\text{M s}^{-1}$, $k_1=40.0 \text{ s}^{-1}$, $k_2=0.02 \text{ s}^{-1}$, $K_0=4.0 \mu\text{M}$, $K_3=0.12 \mu\text{M}$, $K_4=0.12 \mu\text{M}$, $d_a=0.23 \mu\text{M}$, $d_p=1.66 \mu\text{M}$, $d_2=0.6 \mu\text{M}$, $d_1=0.3 \mu\text{M}$, $d_3=0.2 \mu\text{M}$, $V_K=0.075 \mu\text{M s}^{-1}$, $V_{PH}=0.075 \mu\text{M s}^{-1}$, $K_K=1.0 \mu\text{M}$, $K_{PH}=10.0 \mu\text{M}$, $K_d=0.5 \mu\text{M}$, $c=5.0 \mu\text{M s}^{-1}$, $A=1.0 \mu\text{M s}^{-1}$. The parameter V_{PLC} is considered as an important control parameter

and the coupling strength γ is treated as a crucial free parameter. To simulate the dynamical behavior of this model, Eqs. (1)–(4) were integrated by the forward Euler algorithm with a time step of 0.01 s. In each calculation, the time evolution of the system lasted 1000 s after the transient behavior was discarded. The Gaussian noise sources were generated at each integration step by “Minimal” random number generator of Park and Miller with Bays–Durham shuffle and added safeguards [26].

3. Results

To study the synchronization of a population of cells coupled through a mean field, the system studied here is composed of 500 cells with individual structural parameter β .

The calcium dynamics of isolated hepatocytes have been well characterized experimentally. There exists a critical agonist dose above which a hepatocyte responds with regular Ca^{2+} oscillations. From bifurcation diagrams for Ca^{2+} in the coupled multicellular system (data not shown), it can be seen that, intracellular Ca^{2+} oscillations will occur at appropriate value of V_{PLC} and γ .

To investigate effects of the coupling strength γ and V_{PLC} (which reflects the stimulation level) on the synchronization of stochastic Ca^{2+} oscillations, the evolution of x_i for different values of V_{PLC} (Fig. 1) and for different coupling strengths γ (Fig. 2) have been compared. When the stimulation or the coupling is small, only a few cells are induced to oscillate (Figs. 1a or 2a). When the stimulation or the coupling is big enough, all cells are induced to oscillate and become synchronous (see Figs. 1b or 2b). With the increasing of V_{PLC} or of γ further, however, synchrony of this system is weakened (see Figs. 1c or 2c). Figs. 1 and 2 seem to suggest that, there exist optimal stimulation level and coupling strength for the synchronization of this system.

Because that the individual structural parameter of each cell is not identical, a perfect synchronization cannot be achieved and

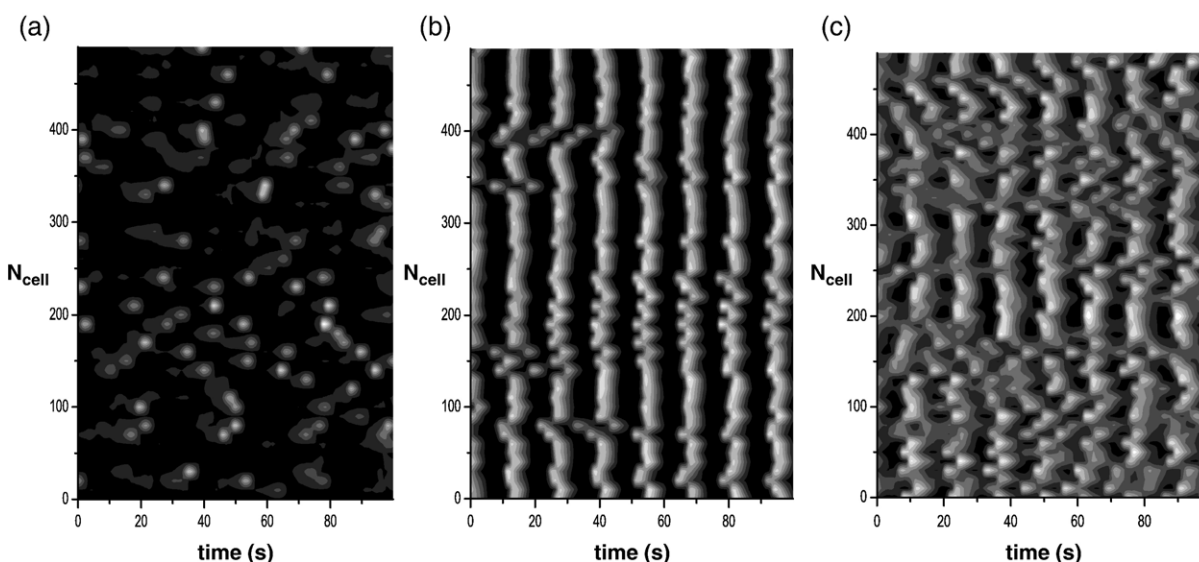


Fig. 1. Snapshots of x_i in 500 cells are shown at three different values of V_{PLC} . The gray scales from black to white represent x_i from 0.1 μM to 1.1 μM . (a) $V_{PLC}=0.012 \mu\text{M s}^{-1}$; (b) $V_{PLC}=0.023 \mu\text{M s}^{-1}$; (c) $V_{PLC}=0.03 \mu\text{M s}^{-1}$. Other parameter values are: $\gamma=1.0 \text{ s}^{-1}$, $M=500$.

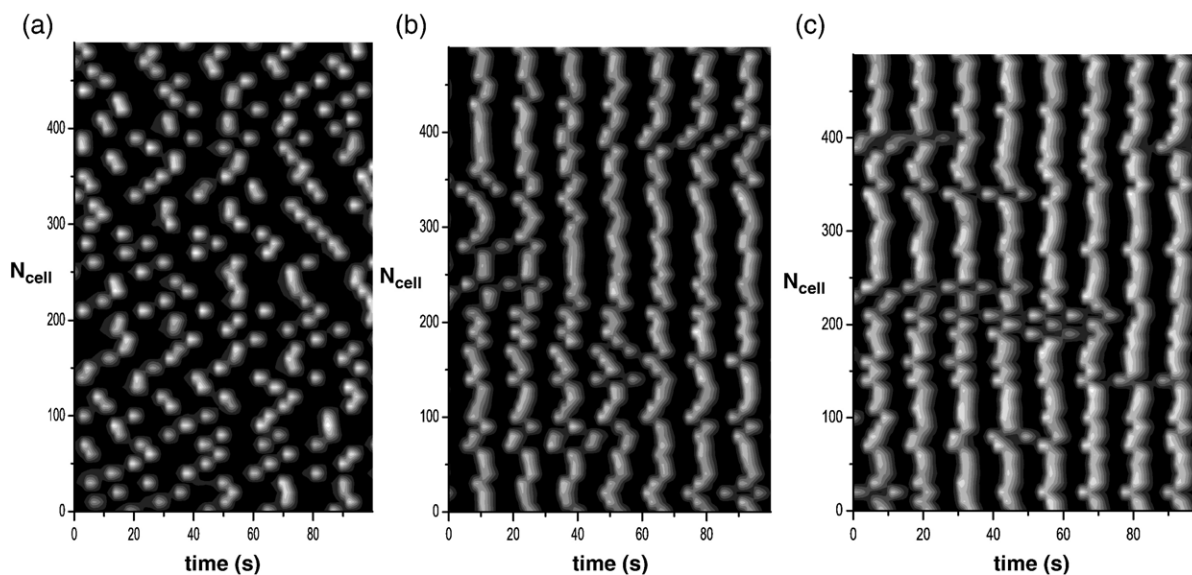


Fig. 2. Snapshots of x_i in 500 cells are shown at three different values of γ . The gray scales from black to white represent x_i from 0.05 μM to 1.1 μM . (a) $\gamma=0.2\text{ s}^{-1}$; (b) $\gamma=1.4\text{ s}^{-1}$; (c) $\gamma=2.1\text{ s}^{-1}$. Other parameter values are: $V_{\text{PLC}}=0.02\text{ }\mu\text{M s}^{-1}$, $M=500$.

phase differences between some oscillators still persist, as observed experimentally. To quantify how good the synchrony is, an order parameter is calculated, which has been used to measure the synchronization of multicellular circadian oscillators [22]:

$$O = \frac{\langle F^2 \rangle - \langle F \rangle^2}{\frac{1}{N} \sum_{i=1}^N (\langle x_i^2 \rangle - \langle x_i \rangle^2)}$$

where $\langle \cdot \rangle$ denotes the average over time. This parameter measures the distribution of phases of oscillations and it is ranging between 0 (no synchronous) and 1 (perfect synchronous, with all oscillators in phase).

The dependence of the order parameter O on V_{PLC} is shown in Fig. 3. In Fig. 3(a), it can be observed that the coupled system shows the strongest order at $V_{\text{PLC}}=0.02\text{ }\mu\text{M s}^{-1}$ when there are 100 IP₃R channels ($M=100$) on ER of each cell, and that the optimal value is $V_{\text{PLC}}=0.023\text{ }\mu\text{M s}^{-1}$ when $M=500$. Furthermore, the peak value of the order parameter O for $M=500$ is bigger than that one for $M=100$. It can be easily understood because that, if the number of IP₃R channels is bigger, the intracellular noise is smaller and then the system is more orderly. However, when $M=10^8$ (close to deterministic case), there is not an obvious peak value of the order parameter O , although O is very big. Fig. 3(b) demonstrates that, if the mean-field coupling strength γ is bigger, the peak value of O is bigger. When the coupling is very small (e.g. $\gamma=0.1\text{ s}^{-1}$), the system that is composed of nearly isolated cells loses the synchronization completely. Moreover, the optimal value of V_{PLC} increases with the decreasing of the coupling strength γ .

Effects of the coupling strength γ on the order parameter O are demonstrated in Fig. 4, in which there exists an optimal coupling strength. Fig. 4(a) is similar to Fig. 3(a). Fig. 4(b) reveals that the optimal coupling strength γ increases with the decreasing of the stimulation level V_{PLC} , which is consistent

with results in Fig. 3(b). There seems to exist cooperation between the coupling strength and the stimulation level.

Figs. 3 and 4 remind us of our previous work [18], which had discussed two and three connected hepatocytes coupled by gap junction. In that paper [18], the cross-correlation time τ_c shows

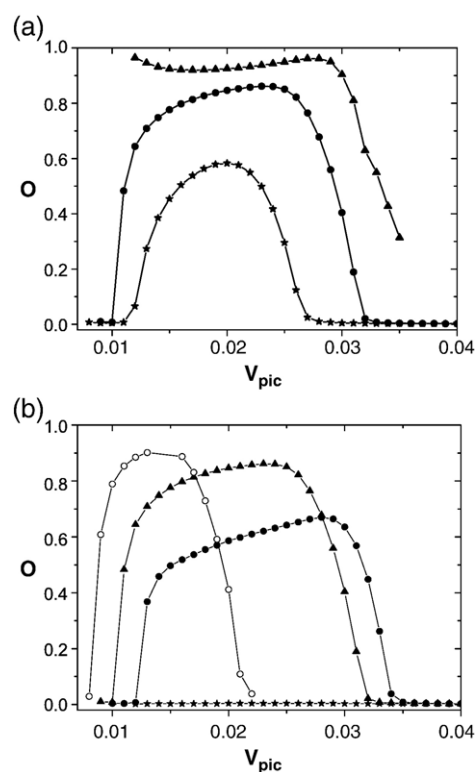


Fig. 3. (a) The order parameter O vs V_{PLC} at a given coupling strength $\gamma=1.0\text{ s}^{-1}$. Star: $M=100$; circle: $M=500$; triangle: $M=10^8$. (b) The order parameter O vs V_{PLC} at $M=500$. Star: $\gamma=0.1\text{ s}^{-1}$; solid circle: $\gamma=0.5\text{ s}^{-1}$; triangle: $\gamma=1.0\text{ s}^{-1}$; open circle: $\gamma=2.0\text{ s}^{-1}$.

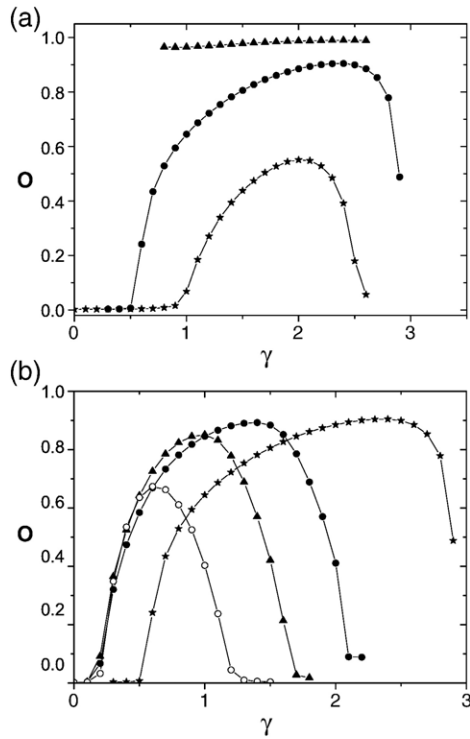


Fig. 4. (a) The order parameter O vs γ at a given $V_{PLC} = 0.012 \mu M s^{-1}$. Star: $M=100$; circle: $M=500$; triangle: $M=10^8$. (b) The order parameter O vs γ at $M=500$. Star: $V_{PLC} = 0.012 \mu M s^{-1}$; solid circle: $V_{PLC} = 0.02 \mu M s^{-1}$; triangle: $V_{PLC} = 0.025 \mu M s^{-1}$; open circle: $V_{PLC} = 0.03 \mu M s^{-1}$.

peak with the increasing of the coupling strength and the IP_3 level, i.e. there exist optimal coupling strength and IP_3 level for the biggest coherence of coupled cells [18]. In fact, results in Figs. 3 and 4 are in agreement with those results in Ref. [18] qualitatively, because that V_{PLC} is the velocity of IP_3 synthesis and it reflects the IP_3 level.

To characterize the synchronization of the coupled multicellular system, a phase is introduced into each cell:

$$\phi_i(t) = 2\pi \frac{t - \tau_k^i}{\tau_{k+1}^i - \tau_k^i} + 2\pi k,$$

The index i denotes the i th cell, $i=1, 2, \dots, N$; the index k denotes the k th spike, $k=1, 2, \dots, K_i$. τ_k^i is the time of the k th spike in the i th cell, which is determined by the threshold value of $x_i(t)$ at $x=0.2 \mu M$. The quantity

$$s_i = \sin^2\left(\frac{\phi_i - \phi_{i+1}}{2}\right),$$

measures the phase synchronization effect of neighboring elements [27]. A spatiotemporal average of s_i , i.e.,

$$S = \lim_{T \rightarrow \infty} \frac{1}{T} \int_0^T dt \left(\frac{1}{N} \sum_{i=1}^N s_i \right), \quad (5)$$

gives a measure of the degree of the phase synchronization in the coupled system. For completely unsynchronized motions $S \approx 0.5$, while for globally synchronized systems $S \approx 0$. Fig. 5

shows the dependence of S upon the coupling strength, which is consistent very well with the result in Fig. 4(a). On the other hand, to test whether these results are correlative with the cells number, the curve for 1000 coupled cells (open circles in Fig. 5) has been plotted, which completely accords with that curve for 500 cells. Therefore, results obtained in this paper can also be applied to other systems with different cells number.

To measure the temporal coherence of noise-induced motion, distribution of pulse duration $T_k^i = \tau_{k+1}^i - \tau_k^i$ are examined. A measurement of the sharpness of the distribution, for example,

$$R = \frac{\langle T_k^i \rangle}{\sqrt{\langle (T_k^i)^2 \rangle - (\langle T_k^i \rangle)^2}}, \quad (6)$$

where

$$\langle (T_k^i)^n \rangle = \frac{\sum_{i=1}^N \sum_{k=1}^{K_i} (T_k^i)^n}{\sum_{i=1}^N K_i}$$

provides an indication of the coherence of spike events. In short, R is the ratio of the average and the standard deviation of the pulse duration and is a kind of signal-to-noise ratio in the sense that periodicity with repetitive firing at fixed pulse duration is a signal [28,29]. It should be noted that R is the reciprocal of the coefficient of variation in a point process that is widely used in the field of neuroscience [30–32]. Biologically, this quantity is of importance because it is related to the timing precision of the information processing in some important systems [33]. Here the same definition has been adopted to measure the coherence of Ca^{2+} oscillations, with the distribution $P(T)$ constructed by pulse durations of all cells during a long enough period of time.

From Fig. 6, it can be observed that, for very weak noise ($M=10^8$), a small coupling strength γ can make the system to gain a high coherence. With the increasing of the noise strength, for all values of the coupling strength, the coherence of spike events is not strong. But there still exists an optimal coupling strength γ whether the noise is big or small.

Although there exist optimal values of V_{PLC} and γ for the most orderly system, there is not an optimal intracellular noise M . Fig. 7 shows that the coupled system is more orderly if the

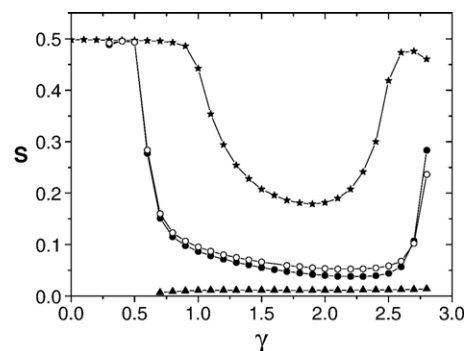


Fig. 5. Degree of the phase synchronization S vs γ at a given $V_{PLC} = 0.012 \mu M s^{-1}$. Star: $M=100, N=500$ cells; solid circle: $M=500, N=500$ cells; triangle: $M=10^8, N=500$ cells; open circle: $M=500, N=1000$ cells.

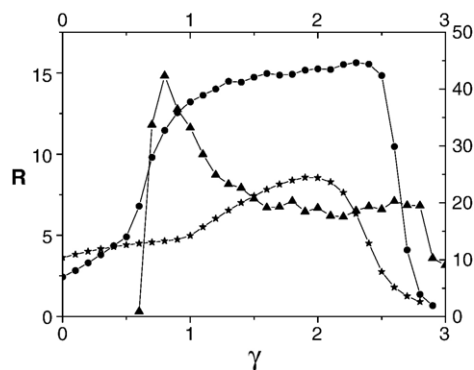


Fig. 6. Signal-to-noise ratio R vs γ at a given $V_{\text{PLC}}=0.012 \mu\text{M s}^{-1}$. Star: $M=100$ (using left axis); circle: $M=500$ (using left axis); triangle: $M=10^8$ (using right axis).

intracellular noise is smaller. In another words, the synchronization of the system always changes monotonically with the intracellular noise. To explore whether effects of an extracellular noise upon the synchronization of the system is the same as that of the intracellular noise, an extracellular noise is introduced into the mean-field F :

$$F(t) = \frac{1}{N} \sum_{i=1}^N x_i(t)(1 + \zeta(t))$$

$\zeta(t)$ is the Gaussian noise with zero mean value and its correlation function is $\langle \zeta(t)\zeta(t') \rangle = D^2 \delta_{tt'}$, where D denotes the extracellular noise intensity. We plot the relationship between S and D in Fig. 8, in which these curves are not monotonous and demonstrate peaks. However there don't exist an optimal extracellular noise, instead, these peak values denote the worst noise strength. For example, when $V_{\text{PLC}}=0.02 \mu\text{M s}^{-1}$, $M=10^8$, the system shows the most disorderly at $D=0.9$. From Figs. 7 and 8, it can be concluded that the intracellular and the extracellular noise play different roles in cells communication. Since the intracellular noise of each cell are independent, they generally tend to disturb a cooperative behavior between cells. However, the extracellular noise are nearly common to all cells due to their common environment, and this has the effect of synchronizing the dynamics of all cells by exerting the same fluctuations on each cell through signal molecules. This view

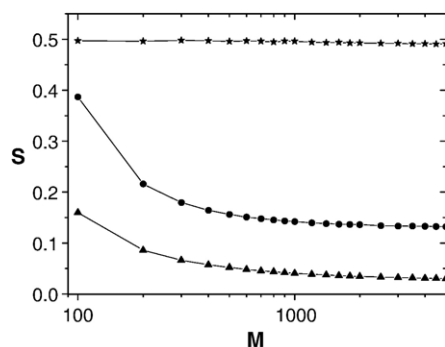


Fig. 7. Degree of the phase synchronization S vs M at a given $V_{\text{PLC}}=0.02 \mu\text{M s}^{-1}$. Star: $\gamma=0.1 \text{ s}^{-1}$; circle: $\gamma=0.5 \text{ s}^{-1}$; triangle: $\gamma=1.0 \text{ s}^{-1}$.

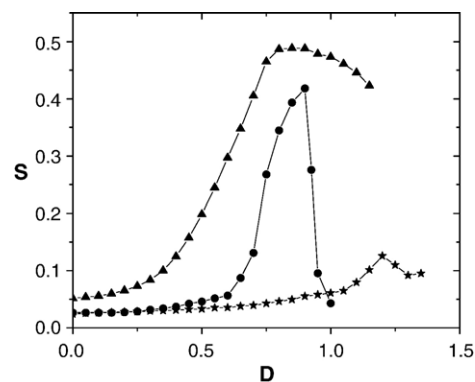


Fig. 8. Degree of the phase synchronization S vs D at a given $\gamma=1.0 \text{ s}^{-1}$. Star: $V_{\text{PLC}}=0.015 \mu\text{M s}^{-1}$, $M=10^8$; circle: $V_{\text{PLC}}=0.02 \mu\text{M s}^{-1}$, $M=10^8$; triangle: $V_{\text{PLC}}=0.02 \mu\text{M s}^{-1}$, $M=500$.

had been brought forward in Ref. [22], and it is worth to discuss this question further in our future work.

4. Conclusions

In this paper, based on Höfer's model and employing stochastic Li–Rinzel model to describe the channel flux, intercellular Ca^{2+} oscillations in coupled hepatocytes have been theoretically explored. In order to study the synchronization of the multicellular system more efficiently, the mean-field coupling instead of the gap junctional coupling has been introduced, which has been used in calcium signal transduction the first time as far as we know.

We compare the evolution of x_i for different values of V_{PLC} (reflecting the stimulation level) (Fig. 1) and for different coupling strengths γ (Fig. 2). The relationship between the degree of the synchronization of oscillations and V_{PLC} or γ is not monotone. Are there optimal stimulation level and coupling strength for the synchronization of this system?

Therefore, an order parameter has been introduced to characterize the degree of the synchronization, which has not been used to analyze the synchronization of Ca^{2+} signal in coupled hepatocytes. Results obtained prove that there exist optimal stimulation level and coupling strength for the synchronization of this system. From Figs. 3 and 4, we can see not only effects of the stimulation level and the coupling strength on the synchronization of the system, but also a cooperative relationship between the stimulation level and the coupling strength. Furthermore, another order parameter S is introduced to characterize the degree of the phase synchronization. And signal-to-noise ratio (i.e., the reciprocal of coefficient of variation) R has been used to measure the coherence of oscillation events. Although the definitions of O , S and R are distinct, the results obtained by them respectively are similar in the extreme (Figs. 4(a), 5, and 6).

Although there exist the optimal value of V_{PLC} and γ for the most orderly system, there is not an optimal intracellular noise M (Fig. 7). The stronger intracellular noise tends to make the system more disorderly. But the extracellular noise introduced from the mean-field has a different effect.

Above analysis suggests that the stimulation level and the coupling strength play important roles in the synchronization of

Ca^{2+} oscillations in a coupled multicellular liver system. This conclusion is qualitatively consistent with our previous work (which described only two and three coupled hepatocytes, [18,19]). Therefore, it can be concluded that it is correct and efficient to apply the mean-field coupling to intercellular Ca^{2+} dynamics in a multicellular system. Furthermore, a comparison between gap junctional coupling in a detailed three dimensional model and mean-field coupling will be a subject of future investigations.

Acknowledgments

This work was supported by the National Natural Science Foundation of China under Grant No. 10575041.

References

- [1] A. Goldbeter, Biochemical Oscillations and Cellular Rhythms. The Molecular Bases of Periodic and Chaotic Behaviour, Cambridge Univ., Press, Cambridge, 1996.
- [2] N.M. Woods, K.S.R. Cuthbert, P.H. Cobbold, Repetitive transient rises in cytoplasmic free calcium in hormone-stimulated hepatocytes, *Nature* 319 (1986) 600–602.
- [3] T.A. Rooney, E.J. Sass, A.P. Thomas, Characterization of cytosolic calcium oscillations induced by phenylephrine and vasopressin in single fura-2-loaded hepatocytes, *J. Biol. Chem.* 264 (1989) 17131–17141.
- [4] A.H. Cornell-Bell, S.M. Finkbeiner, M.S. Cooper, S.J. Smith, Glutamate induces calcium waves in cultured astrocytes: long-range glial signaling, *Science* 247 (1990) 470–473.
- [5] V.A. Golovina, M.P. Blaustein, Spatially and functionally distinct Ca^{2+} stores in sarcoplasmic and endoplasmic reticulum, *Science* 275 (1997) 1643–1648.
- [6] P.D. Koninck, H. Schulman, Sensitive of CaM kinase II to the frequency of Ca^{2+} oscillations, *Science* 279 (1998) 227–230.
- [7] R.E. Dolmetsch, K. Xu, R.S. Lewis, Calcium oscillations increase the efficiency and specificity of gene expression, *Nature* 392 (1998) 933–936.
- [8] G.J. Allen, S.P. Chu, K. Schumacher, C.T. Shimazaki, D. Vafeados, A. Kemper, S.D. Hawke, G. Tallman, R.Y. Tsien, J.F. Harper, J. Chory, J.I. Schroeder, Alteration of stimulus-specific guard cell calcium oscillations and stomatal closing in *Arabidopsis det3* mutant, *Science* 289 (2000) 2338–2342.
- [9] D. Gall, E. Baus, G. Dupont, Activation of the liver glycogen phosphorylase by Ca^{2+} oscillations: a theoretical study, *J. Theor. Biol.* 207 (2000) 445–454.
- [10] D. Wu, Y. Jia, A. Rozi, Effects of inositol 1,4,5-trisphosphate receptor-mediated intracellular stochastic calcium oscillations on activation of glycogen phosphorylase, *Biophys. Chem.* 110 (2004) 179–190.
- [11] A. Rozi, Y. Jia, A theoretical study of effects of cytosolic Ca^{2+} oscillations on activation of glycogen phosphorylase, *Biophys. Chem.* 106 (2003) 193–202.
- [12] T. Tordjmann, B. Berthon, M. Claret, L. Combettes, Coordinated intercellular calcium waves induced by noradrenaline in rat hepatocytes: dual control by gap junction permeability and agonist, *EMBO J.* 16 (1997) 5398–5407.
- [13] T. Tordjmann, B. Berthon, E. Jacquemin, C. Clair, N. Stelly, G. Guillon, M. Claret, L. Combettes, Receptor oriented intercellular waves evoked by vasopressin in rat hepatocytes, *EMBO J.* 17 (1998) 4695–4703.
- [14] C. Clair, C. Chalumeau, T. Tordjmann, J. Poggioli, C. Erneux, G. Dupont, L. Combettes, Investigation of the roles of Ca^{2+} and InsP_3 diffusion in the coordination of Ca^{2+} signals between connected hepatocytes, *J. Cell Sci.* 114 (2001) 1999–2007.
- [15] G. Dupont, T. Tordjmann, C. Clair, S. Swillens, M. Claret, L. Combettes, Mechanism of receptor-oriented intercellular calcium wave propagation in hepatocytes, *FASEB J.* 14 (2000) 279–289.
- [16] Th. Höfer, Model of intercellular calcium oscillations in hepatocytes: synchronization of heterogeneous cells, *Biophys. J.* 77 (1999) 1244–1256.
- [17] M.E. Gracheva, R. Toral, J.D. Gunton, Stochastic effects in intercellular calcium spiking in hepatocytes, *J. Theor. Biol.* 212 (2001) 111–125.
- [18] D. Wu, Y. Jia, X. Zhan, L.J. Yang, Q. Liu, Effects of gap junction to Ca^{2+} and to IP_3 on the synchronization of intercellular calcium oscillations in hepatocytes, *Biophys. Chem.* 113 (2004) 145–154.
- [19] D. Wu, Y. Jia, L.J. Yang, Q. Liu, X. Zhan, Phase synchronization and coherence resonance of stochastic calcium oscillations in coupled hepatocytes, *Biophys. Chem.* 115 (2005) 37–47.
- [20] L.D. Robbgaspers, A.P. Thomas, Coordination of Ca^{2+} signaling by intercellular propagation of Ca^{2+} waves in the intact liver, *J. Biol. Chem.* 270 (1995) 8102–8107.
- [21] M.H. Nathanson, A.D. Burgstahler, A. Mennone, M.B. Fallon, C.B. Gonzalez, J.C. Sáez, Ca^{2+} waves are organized among hepatocytes in the intact organ, *Am. J. Physiol.* 32 (1995) G167–G171.
- [22] D. Gonze, S. Bernard, C. Waltermann, A. Kramer, Spontaneous synchronization of coupled circadian oscillators, *Biophys. J.* 89 (2005) 120–129.
- [23] Y. Li, J. Rinzel, Equations for InsP_3 receptor-mediated $[\text{Ca}^{2+}]_i$ oscillations derived from a detailed kinetic model: a Hodgkin–Huxley like formalism, *J. Theor. Biol.* 166 (1994) 461–473.
- [24] P. Jung, J.W. Shuai, Optimal sizes of ion channel clusters, *Europhys. Lett.* 56 (2001) 29–35.
- [25] G. Dupont, T. Tordjmann, C. Clair, S. Swillens, M. Claret, L. Combettes, Mechanism of receptor-oriented intercellular calcium wave propagation in hepatocytes, *FASEB J.* 14 (2000) 279–289.
- [26] W.H. Press, S.A. Teukolsky, W.T. Vetterling, B.P. Flannery, Numerical Recipes in C, Cambridge University Press, 1992.
- [27] M.G. Rosenblum, A.S. Pikovsky, J. Kurths, Phase synchronization of chaotic oscillators, *Phys. Rev. Lett.* 76 (1996) 1804–1807.
- [28] B. Hu, C. Zhou, Phase synchronization of coupled nonidentical excitable systems and array-enhanced coherence resonance, *Phys. Rev., E* 61 (2000) R1001–R1004.
- [29] Y.J. Shinohara, T. Kanamaru, H. Suzuki, T. Horita, K. Aihara, Array-enhanced coherence resonance and forced dynamics in coupled FitzHugh–Nagumo neurons with noise, *Phys. Rev., E* 65 (2002) 051906-1-7.
- [30] C. Koch, Biophysics of Computation: Information Processing in Single Neurons, Oxford University Press, Oxford, 1999.
- [31] W.R. Softky, C. Koch, The highly irregular firing of cortical cells is inconsistent with temporal integration of 8 random EPSPs, *J. Neurosci.* 13 (1993) 334.
- [32] F. Gabbiani, C. Koch, in: C. Koch, I. Segev (Eds.), Methods in Neural Modeling, MIT Press, Cambridge, MA, 1998.
- [33] X. Pei, L. Wilkens, F. Moss, Noise-mediated spike timing precision from aperiodic stimuli in an array of Hodgkin–Huxley-type neurons, *Phys. Rev. Lett.* 77 (1996) 4679–4682.